

Cite this: *Energy Adv.*, 2024,
3, 778Received 21st January 2024,
Accepted 19th March 2024

DOI: 10.1039/d4ya00038b

rsc.li/energy-advances

A membrane electrode assembly-type cell designed for selective CO production from bicarbonate electrolyte and air containing CO₂ mixed gas†

Akina Yoshizawa,^a Manabu Higashi,^a Akihiko Anzai^a and Miho Yamauchi^{id}*^{abcd}

The electrochemical CO₂ reduction reaction (CO₂RR) combined with direct air capture (DAC) based CO₂ is a promising method for terrestrial carbon cycling. In this study, we have designed an all-Ag cathode and constructed a membrane electrode assembly (MEA) cell to utilize CO₂ capture solution, which can be produced by flowing air containing CO₂ mixed gas into an alkaline solution. A MEA consisting of a Ag nanoparticle catalyst sprayed on a Nafion membrane and a Ag electrode were used to construct a MEA cell (Ag MEA-cell). The Ag MEA-cell exhibited selective CO production without severe side reactions, such as the hydrogen evolution reaction, even when an aqueous electrolyte was used. The operation of the Ag MEA-cell using CO₂ capture solution, which was prepared by bubbling 60% air containing CO₂ mixed gas (40% CO₂ and 60% air, air-CO₂) into 1 M KOH, achieved CO production with 86% faradaic efficiency (FE_{CO}). Furthermore, the Ag MEA-cell significantly suppressed O₂ reduction and achieved FE_{CO} of 74% even when air-CO₂ was used as a CO₂ source.

the past decade, particularly with the development of a gas diffusion electrode (GDE) in fluidized cathode cells and membrane electrode assemblies (MEAs) to improve the activity, product selectivity, and durability of catalysts.^{5–7} Direct air capture (DAC) is one of the attractive methods to extract CO₂ from the air.^{8,9} Currently, several DAC systems have been developed; adsorption-based DAC, which uses an alkaline solvent or a porous solid adsorbent to capture CO₂ as a carbonate/bicarbonate or other CO₂ derivatives, and permeation-based DAC, which consists of a stepwise separation using a membrane (m-DAC).^{10–13} Unlike the other DAC systems, m-DAC does not require the input of large amounts of thermal energy to desorb CO₂ from the adsorbent, although multi-step separation is necessary to produce highly concentrated CO₂. Thus, m-DAC combined with the CO₂RR using impure CO₂ that can be produced by the smaller steps of the m-DAC process, would bypass energy-intensive purification,^{14–16} and dramatically reduce CCU costs; purification of dilute CO₂ gas costs \$70–\$100 per ton (Fig. 1).^{17–20} Meanwhile, when using impure CO₂ containing O₂, the CO₂RR is completely blocked in a conventional flow type cell (Fig. 2a and Fig. S1, ESI†) due to the overwhelmingly superior oxygen reduction reaction (O₂ + 2H₂O + 4e[–] → 4OH[–], ORR) (Fig. S2, ESI†),^{14,21–23} and therefore most of

Introduction

Carbon capture and utilization (CCU) of dilute atmospheric CO₂ and industrial exhaust gas is a key to efficient carbon cycling on earth,^{1,2} and electrochemical CO₂ reduction reactions (CO₂RRs) using captured CO₂ are attracting much attention for the production of chemical feedstocks and fuels from CO₂.^{3,4} The research field of the CO₂RR has evolved substantially over

^a Institute for Materials Chemistry and Engineering (IMCE), Kyushu University, Motoooka 744, Nishi-ku, Fukuoka 819-0395, Japan.
E-mail: yamauchi@ms.ifoc.kyushu-u.ac.jp

^b Advanced Institute for Materials Research (WPI-AIMR), Tohoku University, 2-1-1 Katahira, Aoba-ku, Sendai 980-8577, Japan

^c Research Center for Negative Emissions Technologies (K-NETs), Kyushu University, Motoooka 744, Nishi-ku, Fukuoka 819-0395, Japan

^d International Institute for Carbon-Neutral Energy Research (WPI-I²CNER), Kyushu University, Motoooka 744, Nishi-ku, Fukuoka 819-0395, Japan

† Electronic supplementary information (ESI) available. See DOI: <https://doi.org/10.1039/d4ya00038b>

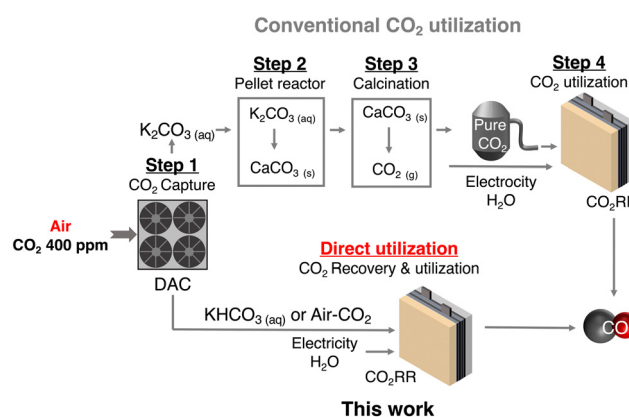


Fig. 1 Scheme of recovery and utilization of atmospheric CO₂.



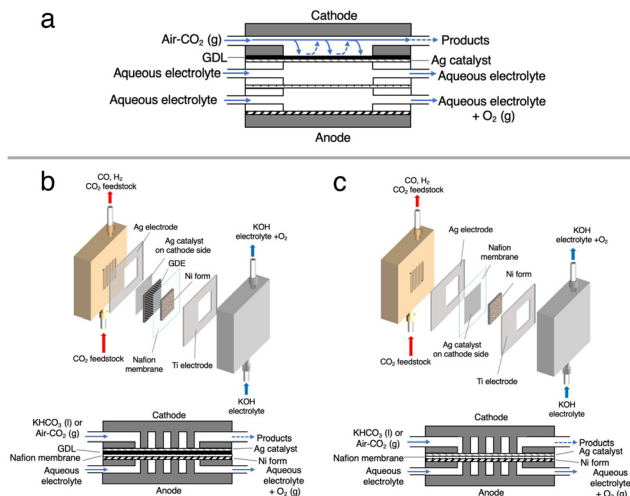


Fig. 2 Side view of (a) a conventional three-chamber cell, (b) the conventional MEA cell using a carbon based GDE and (c) the Ag MEA-cell. Parts with dots, gray oblique lines and black oblique lines are the membrane, cathode anode catalysts and carbon-based GDE, respectively. System configuration of (b) the conventional MEA-cell using GDE and (c) the Ag MEA-cell.

the CO₂RR research has been conducted using pure CO₂ gas (> 99%).^{24–31} Interestingly, direct CO₂RR using air-containing mixed gas has been demonstrated using a newly designed flow cell consisting of a non-carbon gas diffusion layer (GDL),¹⁴ but the products from the mixed gas still contain O₂ and N₂, and should be purified before use.

Recently, the CO₂RR using a bicarbonate solution, which is produced from DAC-captured CO₂ gas, has been in focus as an economically feasible CCU method. Here in this study, we explore efficient CO₂RR using O₂-containing CO₂ mixed gas that is captured by m-DAC. In this system, O₂ and N₂ are first removed by dissolving CO₂ in an alkaline solution to bicarbonate, which can be used as a CO₂ source and electrolyte. However, in a commonly used flow cell equipped with a carbon-based GDL, the HER is largely promoted when the bicarbonate solution is fed because carbon predominantly promotes the HER rather than the CO₂RR (Fig. 2b and Fig. S3, ESI†). To enhance the CO₂RR using a bicarbonate solution, we construct a membrane electrode assembly (MEA)-type cell equipped with two liquid flow channels at both the cathode and the anode. In particular, an all-Ag flow channel MEA cell (Ag MEA-cell) was newly designed for substrate diffusion, cathodic reactions and current collection to avoid severe hydrogen evolution reaction (HER) when aqueous solutions are flowing. We applied KHCO₃ solution prepared by bubbling a CO₂ mixed gas consisting of 40% CO₂ and 60% air (air-CO₂, where CO₂ is enriched by a factor of 1000) into an aqueous 3 M KOH solution. Furthermore, CO₂RR was demonstrated by directly introducing air-CO₂ to Ag MEA-cell.

Experimental section

Materials

The Ag nanoparticles (Ag NPs <100 nm in diameter) and Nafion™ perfluorinated resin solution (5 wt% in a mixture of low aliphatic alcohols and H₂O, containing 45% H₂O) were

purchased from Sigma-Aldrich Co. LLC. Isopropanol (> 99.7%), KHCO₃ (99%), KOH (> 85%), and K₂CO₃ (99%) were obtained from FUJIFILM Wako Pure Chemical Corporation. All chemicals were used as received without further purification. Nafion™ 117 membrane was provided by Chemours. The Ag sheet and the titanium foil were purchased from the Nilaco Corporation. Nickel foam (1.6 mm thick, purity > 99.99%) was obtained from MTI Corporation. Oxygen (> 99.9%), CO₂ (> 99.5%), and N₂ (> 99.9%) were provided by Fukuoka Oxygen Co., Ltd.

Preparation of MEA and construction of a flow cell

Cathode electrodes were prepared using a reported air-brushing method.²⁷ Cathodic catalyst ink was prepared by mixing Ag NPs (40 mg), isopropanol (200 μL), deionized H₂O (50 μL), and Nafion™ perfluorinated resin solution (80 μL). The ink was airbrushed to a piece of Nafion™ 117 membrane, and allowed to air dry naturally. Unless otherwise noted, the Ag NP-sprayed cathodes were prepared with a catalyst loading of 2.5 mg cm⁻². Then, the MEA consisted of a nickel foam anode and a Ag NP-sprayed Nafion™ 117 membrane was prepared (Ag-MEA, Fig. 2c). A Ag MEA-cell was constructed by placing Ag-MEA between a Ag cathode and a Ti anode, with a polyether-etherketone (PEEK) flow plate on the cathode side and a Ti-based flow plate on the anode side. Each electrode was surrounded by silicone rubber for electrical insulation and to seal each compartment.

Characterizations

The morphology of the electrodes was evaluated by scanning electron microscopy (SEM) using a JSM-IT100 (JEOL) at 15 kV. The structures of the electrodes were identified by powder X-ray diffraction (XRD) using a D2 Phaser (Bruker).

The electrochemical measurement

Electrocatalytic measurements were performed with an electrochemical test system 1280Z (Solartron) in a two-electrode setup (Fig. 2c). 1.0 M KOH aqueous solution was used as the anolyte and fed to the anode compartment of the Ag MEA-cell at a flow rate of 1.0 mL min⁻¹. The cathode compartment was fed with KHCO₃ solution (BCS) at a flow rate of 1.0 mL min⁻¹ or reactant gases at a flow rate of 15 ccm. The current density (*j*) on Ag MEA-cell was calculated based on the Ag cathode area covering Ag-MEA. Gas products were quantified by using a Micro GC FUSION (INFICON). The absence of liquid product was confirmed by high performance liquid chromatography (HPLC) using LC-20AD (Shimadzu) equipped with an RID-10A refractive index detector (Shimadzu). From gas chromatography (GC) and HPLC, no products other than CO and H₂ were detected by GC or HPLC. Resistance values for Ag MEA-cells were measured using the 1280Z electrochemical test system. The faradaic efficiencies (FE) were investigated in the cell voltage range of 1.8 to 2.4 V. The FEs for the production of CO (FE_{CO}) and H₂ (FE_{H₂}) were calculated according to the report and the representative results in several experimental tests are shown in this paper.²⁹ Because the size of the cell components was nearly



identical, the measured resistances without iR correction were directly used for discussion.

Results and discussion

CO₂RR using a bicarbonate solution

We first tested the CO₂RR on a typical MEA cell (Fig. 2b) with Ag NPs applied on a carbon-based gas diffusion electrode (GDE). Chronoamperometry was conducted by flowing 1.0 M BCS as a simulated CO₂-captured solution to the cathode side at a flow rate of 1.0 mL min⁻¹ and 1.0 M KOH to the anode side at a flow rate of 1.0 mL min⁻¹. Fig. S3 (ESI[†]) represents that the FE_{H₂} and FE_{CO} values on the MEA cell at 2.0 V of the cell voltage are 16 and 63%, respectively, indicating that the CO₂RR can proceed on a carbon-based GDE although the HER is still not negligible in the voltage range between 2.0 and 2.6 V.^{26,32} It should be noted that the total FE did not reach 100% because of the difficulty in precisely controlling H₂ uptake at relatively low potentials in our experimental setup. At a voltage higher than 2.4 V, the HER was further promoted. Several authors have reported that a high overpotential is required to initiate the CO₂RR on the carbon-based GDE where the HER is predominant,^{14,33} and therefore, we constructed a Ag MEA-cell without using a carbon-based GDE (Fig. 2c). Two flow plates with serpentine channels were used to supply 1.0 M KOH and 1.0 M BCS to the anode and the cathode, respectively. We used a PEEK channel to flow BCS on the cathode side because metal electrodes usually promote the HER in CO₂RR conducted in an aqueous electrolyte.^{34,35} In addition, a Ag sheet with a square window was used as the electrode on the cathode side to minimize the contact between the electrode and electrolyte solution (Fig. 2c and 3a). SEM observation confirmed that the surface of the Nafion membrane was uniformly covered with Ag NPs without delamination and significant agglomeration (Fig. 3b–d).

We evaluated the CO₂RR performance of the Ag MEA-cell using BCS and found that CO and H₂ were the only detectable cathodic products based on the analysis of the outlet gas and electrolyte at the cathode compartment. The SEM images of the cathode side of the MEA before and after the reaction showed minimal change in surface morphology during the reaction (Fig. 3c and d). The X-ray diffraction (XRD) pattern of the Ag NPs on the starting MEA indicated characteristic peaks at 38.3, 44.5, 64.7 and 77.7°, corresponding to diffractions from the (111), (200), (220) and (311) planes of Ag, respectively and there was no change in the XRD patterns of the Ag NPs on the MEA before and after the reaction. These results confirmed that the Ag NPs on the cathode maintained their structure under our experimental conditions (Fig. S4 and Table S1, ESI[†]).

Fig. S5a (ESI[†]) shows the *J*, FE_{CO} and FE_{H₂} in the CO₂RR using 1 M BCS in the voltage range between 1.8 and 2.4 V. As the cell voltage increased, the *J* gradually increased from 12.2 mA cm⁻² at 1.8 V to 59.0 mA cm⁻² at 2.4 V. Thus, the CO₂RR using BCS was achieved at voltages much lower than 3.0 V and previously reported voltages using a bipolar membrane (BPM).^{36–38} At 2.0 V, FE_{H₂} became minimal (FE_{H₂} = 9.2%),

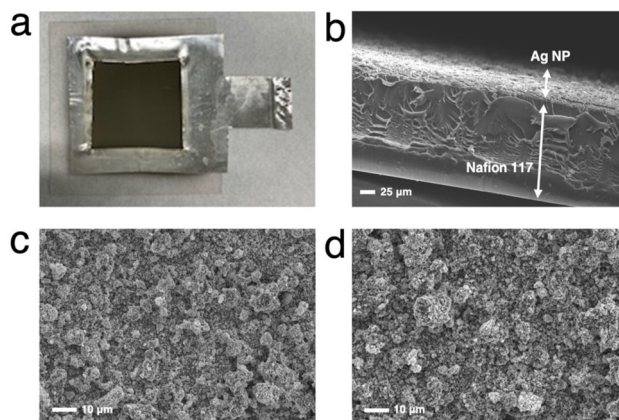


Fig. 3 (a) A photograph of the MEA for the Ag MEA-cell and (b) the cross-section SEM image of the MEA with 2.5 mg cm⁻² of Ag NPs. SEM images of the Ag NPs coated on the MEA (c) before and (d) after the CO₂RR in BCS.

whereas FE_{CO} increased to FE_{CO} = 93% with *J* = 27 mA cm⁻², suggesting that a more selective CO₂RR occurs compared to those on MEA cells with a carbon-based GDE (FE_{H₂} = 16% and FE_{CO} = 63% with *J* = 30.9 mA cm⁻² at 2.0 V, Fig. S3, ESI[†]). Considering that 3 M BCS is the almost saturated one, we performed the CO₂RR using 2 M and 3 M BCSs to increase the efficiency (Fig. 4a and Fig. S5b, ESI[†]). When 2 M BCS was flowed, we achieved the best performance with FE_{CO} > 99% and *J* = 51.5 mA cm⁻² at 2.1 V (Fig. 4a), indicating that almost pure CO was obtained as a CO₂RR product. The high selectivity and good *J* in the CO₂RR using 2 M BCS are possibly related to the appropriate balance between the BCS concentration and the solution resistances; 1, 2 and 3 M BCS showed resistances of 1.31, 2.17 and 3.08 Ω, respectively. A comparison of the performance found here with the reported results is summarized in Table S3 (ESI[†]).

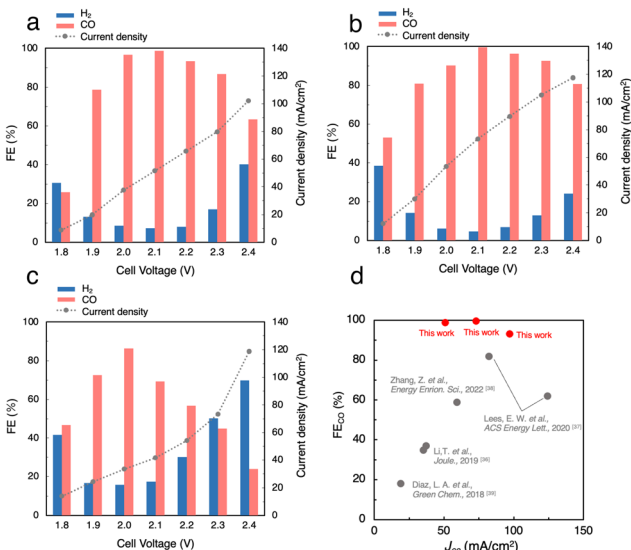


Fig. 4 Faradaic efficiency (FE) and current density (*J*) for the CO₂RR using (a) 2.0 M BCS and (b) CO₂-sol and (c) air-CO₂-sol. (d) Comparison of state-of-the-art performances for the CO₂RR using BCS coupled with CO₂ capture.



CO₂RR using a CO₂ capture solution

Next, we performed the CO₂RR by flowing a CO₂ capture solution, which was prepared by bubbling pure CO₂ gas into 1.0 M KOH (CO₂-sol, pH 7.55, Table S2, ESI[†]) as the electrolyte, and achieved FE_{CO} > 99% and $J = 73.3 \text{ mA cm}^{-2}$ at 2.1 V (Fig. 4b). Interestingly, FE_{CO} remained at 93% even with a relatively high $J = 105 \text{ mA cm}^{-2}$ at 2.3 V, which implies that the J values in the CO₂RR using CO₂-sol are higher than those in BCSs. The reported MEA cells using BCS mostly used a BPM, which requires a large overpotential of more than 3.0 V for the dissociation of H₂O into H⁺ and OH⁻ at the membrane (H₂O(l) \rightleftharpoons H⁺(aq) + OH⁻(aq)).^{36–38} In contrast, our Ag MEA-cell made of a Nafion membrane can eliminate the need for H₂O dissociation. Furthermore, the Ag MEA-cell showed higher FE_{CO} and higher J compared to the previously reported performances, which exhibits great potential of CO₂RRs for the direct utilization of BCS as a CO₂ resource.^{36–39}

We then demonstrated the CO₂RR using a CO₂ capture solution prepared by bubbling air-CO₂ into 3 M KOH (air-CO₂-sol). The pH of air-CO₂-sol was 7.90 (Table S2, ESI[†]), indicating that bicarbonate is the primary carbon species in air-CO₂-sol.⁴⁰ A high FE_{CO} of 86% with $J = 33.4 \text{ mA cm}^{-2}$ in the CO₂RR using air-CO₂-sol was realized at 2.0 V (Fig. 4c), indicating that the Ag MEA-cell exhibits significantly high selectivity for CO production even using air-CO₂-sol and a high possibility for direct utilization of various impure CO₂ sources.

CO₂RR using 60% air containing CO₂

We tried to directly apply air-CO₂ as a reactant gas to Ag MEA-cell. As mentioned above, the inclusion of O₂ in the reactant gas is known to completely inhibit the progress of the CO₂RR in a conventional electrochemical flow cell due to highly preferential ORR.^{14,22} In fact, we performed the CO₂RR by feeding air-CO₂ into a conventional flow cell using a carbon-based GDE on which Ag NPs were applied (Fig. 2a and Fig. S1, ESI[†]),^{23,26,32} but did not observe any products, neither CO nor H₂ (Fig. S2, ESI[†]). This result implies that CO₂ does not interact with the Ag catalyst on the carbon GDE in the presence of air and that the current flowing into the GDE is predominantly used for the ORR before the onset of the CO₂RR, which is explained by the fast kinetics of the ORR.^{41–44} It should be recalled that the newly designed Ag MEA-cell has a unique structure in which the reactant gas can directly contact the Ag NP catalyst, implying the possibility of the CO₂RR on Ag MEA-cell even with air-CO₂. Before investigating the CO₂RR with air-CO₂, the CO₂RR performance on the Ag MEA-cell was examined by flowing pure CO₂ to the cathode side. Fig. S6 (ESI[†]) represents that J increases with increasing cell voltage, reaching 100 mA cm⁻² at 2.3 V and the CO₂RR using pure CO₂ gas shows more than 2 times better J between 2.0 and 2.4 V compared to the CO₂RR using 1 M BCS. The voltage was considerably small compared to the reported voltage of 3.5 V on a BPM-equipped MEA cell showing the large overpotential on a BPM to dissociate H₂O into H⁺ and OH⁻.^{45–47} Furthermore, we achieved FE_{CO} = 97% at 2.3 V and $J = 100 \text{ mA cm}^{-2}$ using the optimized Nafion loading on Ag-MEA (Fig. S7 and S8a, ESI[†]).

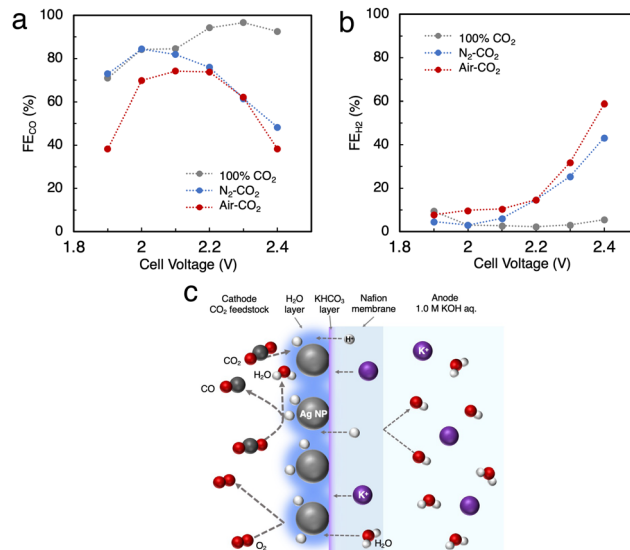


Fig. 5 (a) FE for CO production (FE_{CO}) and (b) for the HER (FE_{H₂}) in the CO₂RR using N₂-CO₂ and air-CO₂. (c) Predicted mechanism of the CO₂RR on the Ag MEA-cell.

To investigate the effect of CO₂ concentration, we used a mixed gas consisting of 40% CO₂ and 60% N₂ (N₂-CO₂) for the CO₂RR in the voltage range of 2.0 to 2.4 V with 10% Nafion loading on Ag-MEA under the optimized conditions (Fig. S8b, ESI[†]). We found that the selectivity for the CO₂RR is significantly reduced when using N₂-CO₂, especially at higher cell voltages above 2.3 V (Fig. 5a and b). For example, the FE_{CO} was reduced to 48% at 2.4 V compared to FE_{CO} = 93% at 2.4 V for pure CO₂, whereas FE_{H₂} was significantly increased to 43%, suggesting that the HER is promoted at low CO₂ concentration.

Subsequently, air-CO₂ was used as a CO₂ source to examine the effect of O₂ inclusion on the CO₂RR. The CO₂RR in the Ag MEA-cell reached FE_{CO} = 74% and $J = 56.7 \text{ mA cm}^{-2}$ at 2.2 V (Fig. S8c, ESI[†]), which is analogous to FE_{CO} = 76% and $J = 39.9 \text{ mA cm}^{-2}$ at 2.2 V for N₂-CO₂ (Fig. S8b, ESI[†]), indicating that the decrease in FE_{CO} is caused by the low CO₂ concentration, not by the enhancement of the ORR. When the CO₂RR was performed above 1.9 V, the total FE values or the sum of FE_{CO} and FE_{H₂} became less than 100%, which suggests that a part of the flowed current is used for the ORR, and the HER was increased above 2.3 V. Thus, the favorable FE_{CO} in the CO₂RR with using air-CO₂ between 2.0 and 2.2 V is possibly explained by the previously reported phenomenon,⁴² a thin layer of H₂O is formed on the Ag catalyst surface by the ORR, which prevents O₂ from contacting the Ag catalyst surface as shown in Fig. 5c. In addition, the H₂O produced by the ORR increases the moisture content of the Nafion membrane, which reduces its insulating properties and results in a relatively high J value.

Conclusion

The newly constructed Ag MEA-cell significantly suppresses the HER, which makes it applicable to the CO₂RR using BCS.



Table 1 The summary of the CO₂RR results using various CO₂ sources

Entry	CO ₂ source	Cell voltage (V)	FE _{CO} (%)	<i>J</i> (mA cm ⁻²)
1	2 M BCS	2.1	>99	51.5
2	CO ₂ -sol	2.1	>99	73.3
3	Air-CO ₂ -sol	2.0	86	33.4
4	CO ₂	2.3	97	100
5	Air-CO ₂	2.2	74	56.7

After the detailed optimization of the reaction conditions, we have achieved the maximum FE_{CO} > 99% and partial current density for CO production (*J*_{CO}) of 73.3 mA cm⁻² in the CO₂RR using 1.0 M CO₂-sol. Even when we used air-CO₂-sol, high CO selectivity FE_{CO} = 86% with 33.4 mA cm⁻² was achieved at 2.0 V (Table 1). Furthermore, excellent CO selectivity with FE_{CO} = 74% and relatively high *J* = 52.7 mA cm⁻² were realized by direct application of air-CO₂ to Ag MEA-cell, suggesting a selective CO₂RR with suppressed ORR even using air-CO₂ due to the unique structure of the Ag MEA-cell where the contact points between air-CO₂ and the electrode were minimized. These results showed that the Ag MEA-cell structure has high potential for the direct conversion of CO₂ feedstocks captured by DAC, which would broaden the applicability of the combination of DAC and CO₂RR technologies.

Author contributions

A. Y. and M. H. designed the experiments and M. Y. supervised the project. M. H. performed the electrolyzer experiments. A. A and A. Y. measured XRD, and A. A., A. Y. and M. H. measured SEM of the MEAs. A. Y. and M. H. defined the reactions in the flow cell. A. Y. performed the data analysis. A. Y. wrote the first manuscript draft and all authors contributed to manuscript writing.

This work was supported by NEDO the Moonshot Research and Development Program (JPNP18016) and JSPS KAKENHI (JP22K19088, JP23H00313).

Conflicts of interest

The authors declare no competing financial interest.

Notes and references

- 1 J. Artz, T. E. Müller, K. Thenert, J. Kleinekorte, R. Meys, A. Sternberg, A. Bardow and W. Leitner, *Chem. Rev.*, 2018, **118**, 434–504.
- 2 H.-J. Ho, A. Iizuka and E. Shibata, *Ind. Eng. Chem. Res.*, 2019, **58**(21), 8941–8954.
- 3 J. Qiao, Y. Liu, F. Hong and J. Zhang, *Chem. Soc. Rev.*, 2014, **43**, 631–675.
- 4 O. G. Sánchez, Y. Birdja, M. Bulut, J. Vaes, T. Breugelmans and D. Pant, *Curr. Opin. Green Sustainable Chem.*, 2019, **16**, 47–56.
- 5 G. Díaz-Sainz, M. Alvarez-Guerra, B. Ávila-Bolívar, J. Solla-Gullón, V. Montiel and A. Irabien, *J. Chem. Eng.*, 2021, **405**, 126965.
- 6 W. Lee, Y. E. Kim, M. H. Youn, S. K. Jeong and K. T. Park, *Angew. Chem., Int. Ed.*, 2018, **57**, 6883–6887.
- 7 Y. C. Li, G. Lee, T. Yuan, Y. Wang, D.-H. Nam, Z. Wang, F. P. García de Arquer, Y. Lum, C.-T. Dinh, O. Voznyy and E. H. Sargent, *ACS Energy Lett.*, 2019, **4**(6), 1427–1431.
- 8 E. S. Sanz-Pérez, C. R. Murdock, S. A. Didas and C. W. Jones, *Chem. Rev.*, 2016, **116**(19), 11840–11876.
- 9 A. Sodiq, Y. Abdullatif, B. Aissa, A. Ostovar, M. Nassar, M. El-Naas and A. Amhamed, *Environ. Technol. Innov.*, 2023, **29**, 102991.
- 10 O. Selyanchyn, R. Selyanchyn and S. Fujikawa, *ACS Appl. Mater. Interfaces*, 2020, **12**(29), 33196–33209.
- 11 S. Fujikawa, R. Selyanchyn and T. Kunitake, *Polym. J.*, 2021, **53**, 111–119.
- 12 S. Fujikawa and R. Selyanchyn, *MRS Bull.*, 2022, **47**, 416–423.
- 13 R. Castro-Muñoz, M. Z. Ahmad, M. Malankowska and J. Coronas, *J. Chem. Eng.*, 2022, **446**(2), 137047.
- 14 A. Anzai, M. Higashi and M. Yamauchi, *Chem. Commun.*, 2023, **59**, 11188–11191.
- 15 D. M. D'Alessandro, B. Smit and J. R. Long, *Angew. Chem., Int. Ed.*, 2010, **49**, 6058–6082.
- 16 M. E. Boot-Handford, J. C. Abanades, E. J. Anthony, M. J. Blunt, S. Brandani, N. Mac Dowell, J. R. Fernández, M.-C. Ferrari, R. Gross, J. P. Hallett, R. S. Haszeldine, P. Heptonstall, A. Lyngfelt, Z. Makuch, E. Mangano, R. T. J. Porter, M. Pourkashanian, G. T. Rochelle, N. Shah, J. G. Yao and P. S. Fennell, *Energy Environ. Sci.*, 2014, **7**, 130–189.
- 17 M. T. Ho, G. W. Allinson and D. E. Wiley, *Energy Procedia*, 2009, **1**, 763–770.
- 18 R. F. Service, *Science*, 2016, **354**, 1362–1363.
- 19 B. Kim, S. Ma, H.-R. M. Jhong and P. J. A. Kenis, *Electrochim. Acta*, 2015, **166**, 271–276.
- 20 M. Erans, E. S. Sanz-Pérez, D. P. Hanak, Z. Clulow, D. M. Reiner and G. A. Mutch, *Energy Environ. Sci.*, 2022, **15**, 1360–1405.
- 21 D. Kim, W. Choi, H. W. Lee, S. Y. Lee, Y. Choi, D. K. Lee, W. Kim, J. Na, U. Lee, Y. J. Hwang and D. H. Won, *ACS Energy Lett.*, 2021, **6**, 3488–3495.
- 22 S. Polani, N. Kanovsky and D. Zitoun, *ACS Appl. Nano Mater.*, 2018, **1**, 3075–3079.
- 23 F. Li, C. Zhou, E. Feygin, P.-N. Roy, L. D. Chen and A. Klinkova, *Phys. Chem. Chem. Phys.*, 2022, **24**, 19432–19442.
- 24 M. R. Thorson, K. I. Siil and P. J. A. Kenis, *J. Electrochem. Soc.*, 2013, **160**, F69.
- 25 B. Kim, S. Ma, H.-R. M. Jhong and P. J. A. Kenis, *Electrochim. Acta*, 2015, **166**, 271–276.
- 26 S. Ma, R. Luo, J. I. Gold, A. Z. Yu, B. Kim and P. J. A. Kenis, *J. Mater. Chem. A*, 2016, **4**(22), 8573–8578.
- 27 S. Ma, M. Sadakiyo, R. Luo, M. Heima, M. Yamauchi and P. J. A. Kenis, *J. Power Sources*, 2016, **301**, 219–228.
- 28 S. Ma, M. Sadakiyo, M. Heima, R. Luo, R. T. Haasch, J. I. Gold, M. Yamauchi and P. J. A. Kenis, *J. Am. Chem. Soc.*, 2017, **139**(1), 47–50.
- 29 A. Anzai, M.-H. Liu, K. Ura, T. G. Noguchi, A. Yoshizawa, K. Kato, T. Sugiyama and M. Yamauchi, *Catalysts*, 2022, **12**, 478.



- 30 M. Sun, A. Staykov and M. Yamauchi, *ACS Catal.*, 2022, **12**(24), 14856–14863.
- 31 M. Sun, J. Cheng and M. Yamauchi, *Nat. Commun.*, 2024, **15**, 491.
- 32 Q. Lu, J. Rosen, Y. Zhou, G. S. Hutchings, Y. C. Kimmel, J. G. Chen and F. Jiao, *Nat. Commun.*, 2014, **5**, 3242.
- 33 K. Yang, R. Kas, W. A. Smith and T. Burdyny, *ACS Energy Lett.*, 2021, **6**, 33–40.
- 34 Y. Hori, H. Wakebe, T. Tsukamoto and O. Koga, *Electrochim. Acta*, 1994, **39**, 1833–1839.
- 35 Y. J. Sa, C. W. Lee, S. Y. Lee, J. Na, U. Lee and Y. J. Hwang, *Chem. Soc. Rev.*, 2020, **49**, 6632–6665.
- 36 T. Li, E. W. Lees, M. Goldman, D. A. Salvatore, D. M. Weekes and C. P. Berlinguette, *Joule*, 2019, **3**, 1487–1497.
- 37 E. W. Lees, M. Goldman, A. G. Fink, D. J. Dvorak, D. A. Salvatore, Z. Zhang, N. W. X. Loo and C. P. Berlinguette, *ACS Energy Lett.*, 2020, **5**, 2165–2173.
- 38 Z. Zhang, E. W. Lees, F. Habibzadeh, D. A. Salvatore, S. Ren, G. L. Simpson, D. G. Wheeler, A. Liu and C. P. Berlinguette, *Energy Environ. Sci.*, 2022, **15**, 705–713.
- 39 L. A. Diaz, N. Gao, B. Adhikari, T. E. Lister, E. J. Dufek and A. D. Wilson, *Green Chem.*, 2018, **20**, 620–626.
- 40 J. Zosel, W. Oelßner, M. Decker, G. Gerlach and U. Guth, *Meas. Sci. Technol.*, 2011, **22**, 072001.
- 41 M. Chatenet, L. Genies-Bultel, M. Aurousseau, R. Durand and A. Andolfatto, *J. Appl. Electrochem.*, 2002, **32**, 1131–1140.
- 42 L. Tammeveski, H. Erikson, A. Sarapuu, J. Kozlova, P. Ritslaid, V. Sammelselg and K. Tammeveski, *Electrochem. Commun.*, 2012, **20**, 15–18.
- 43 Z. Chen, C. Li, Y. Ni, F. Kong, Y. Zhang, A. Kong and Y. Shan, *Electrochim. Acta*, 2017, **239**, 45–55.
- 44 H. Erikson, A. Sarapuu and K. Tammeveski, *ChemElectroChem*, 2019, **6**, 73–86.
- 45 D. A. Salvatore, D. M. Weekes, J. He, K. E. Dettelbach, Y. C. Li, T. E. Mallouk and C. P. Berlinguette, *ACS Energy Lett.*, 2018, **3**, 149–154.
- 46 C. P. O'Brien, R. K. Miao, S. Liu, Y. Xu, G. Lee, A. Robb, J. E. Huang, K. Xie, K. Bertens, C. M. Gabardo, J. P. Edwards, C.-T. Dinh, E. H. Sargent and D. Sinton, *ACS Energy Lett.*, 2021, **6**, 2952–2959.
- 47 K. Yang, M. Li, S. Subramanian, M. A. Blommaert, W. A. Smith and T. Burdyny, *ACS Energy Lett.*, 2021, **6**, 4291–4298.

